Electronic Supplementary Material (ESI) for Energy & Environmental Science.

Supplementary Materials

Bio-inspired organic cobalt(II) phosphonates toward water oxidation

*Tianhua Zhou, Danping Wang, Simon Chun-Kiat Goh, Jindui Hong, Jianyu Han, Jianggao Mao*and Rong Xu**

Material

All solvents and chemicals are obtained from commercial supplies and used directly as received unless otherwise stated. [Ru(2,2'-bipyridine)$_3$]Cl$_2$, 3-phosphonopropionic acid (PPAH$_3$), phenylphosphonic acid (PPH$_3$) and sodium tetraboratedecahydrate were purchased from Sigma-Aldrich. $Na_2S_2O_8$ was obtained from Alfa Aesar.$^{18}OH_2$ solution (97%) was purchased from Cambridge Isotopes Labs. *N*-(phosphonomethyl)proline (S-H$_3$L)[S1] were prepared according to the procedures in our previous reports. Co_3O_4 nanocrystals were synthesized according to the reported method.[S2,S3]

Methods

Characterization

Elemental analysis (C, H, N) was performed on an Elementary Vario El III instrument. FT-IR spectra were obtained with a Perkin Elmer FT-IR Spectrum GX using KBr technique in the range of 4000–400 cm^{-1}. Thermogravimetric analyses (TGA) were carried out with a TA Intruments TGA 5000 instrument at a heating rate of 15 °C/min under air atmosphere. Powder X-ray diffraction (XRD) patterns were obtained on a Bruker AXS D2 Advanced X-ray diffractometer with monochromatized Cu Ka radiation (λ = 1.54056 Å, 40 kV and 20 mA). The data were collected with 2θ in a range of 5°-65° and a step size of 0.02°/0.5 s. All measurements were performed at room temperature and atmospheric pressure. UV-Vis diffuse reflectance spectra (DRS) were obtained by UV-visible absorption spectroscopy (UV-

2450, Shimadzu). The chemical state of cobalt was analyzed by means of XPS analysis performed on a VG Escalab 220iXL and the binding energies were calibrated using the C 1s peak at 285.0 eV. TEM was performed on transmission electron microscopy (TEM, JEOL JEM-3010 and JEM-2100). BET surface areas of both as-synthesized crystal samples (without grinding) and grinded samples were measured by N_2 adsorption and desorption at 77 K using a Quantachrome Autosorb-6 sorption system. Samples were degassed offline at 100 °C or 80 °C for 20 h under vacuum before the analysis. Inductively coupled plasma mass spectrometry was performed with an Agilent 7700x-MS Inductively Coupled Plasma-Mass Spectrometer (ICP-MS). Samples were prepared as described for photocatalytic water oxidation. The solid samples were removed from the solution with 20 min of centrifugation at 20,000 rpm after visible-light irradiation for 80 min. The remaining solution was used for analysis.

Fluorescence spectra

Fluorescence spectra of 1 mM $[Ru(2,2'\text{-bipyridine})_3]Cl_2$ dissolved in 40 mM borate buffer (pH 9.0) in the absence and presence of 5 mM $Na_2S_2O_8$ were collected on a Fluoromax-3 spectrometer (Horiba Scientific). The latter solution was further added with the catalyst (**1** and Co_3O_4, 0.14 g L^{-1}) for fluorescence study.

Electrochemistry

The electrochemical measurements were carried out on a CHI660C electrochemical workstation (CH Instruments, Shanghai Chenghua Co.) with a conventional three-electrode cell consisting of a Pt plate as the counter electrode. The Ag/AgCl (3 M KCl filled) was used as the reference electrode. Electrochemical data were adjusted to NHE by adding 0.197 V to the potential measurements. Solutions of 0.1 M electrolyte were prepared by mixing appropriate volumes of 0.1 M KH_2PO_4 and 0.1

M K_2HPO_4 and the pH of the solution was adjusted to desired values by titrating with 0.1 M HNO_3 or KOH aqueous solution. The pH was measured with a digital pH meter (Sartorius DOCU). The working electrode was prepared as following. A glassy carbon electrode was polished with 0.05μm Al_2O_3.Then the electrode was ultrasonicated in deionized water, ethanol and acetone, followed by drying at room temperature. An appropriate weight of cobalt phosphonates (5 mg) was dispersed in a mixture of 16 μL of 5 wt% Naphthol ethanol solution, 250 μL of 2-propanol and 750 μL of water followed by homogenization using a ultrasonication. Then 10 μL of the catalyst suspension was loaded on a glassy carbon electrode of 5 mm rotating disk electrode (RDE) (loading about 0.25 mg cm^{-2}) and dried in air at room temperature. Prior to measurement, the electrolyte was thoroughly bubbled by purging it with oxygen. Then the RDE was subjected to potential cycling (0.4 to 1.54 V vs NHE, 100 mV/s) in 0.1 M phosphate buffer solution (pH 7) at least 40 cycles before cyclic voltammetry (CV) were recorded at a scan rate of 20 mV/s with rotating rate of 1600 rpm. Linear sweep voltammetry (LSV) was obtained with a scan rate of 2 mV/s, which was also used to collect the Tafel data. The resistance collected was used to correct the Tafel plot for iR drop. Overpotential η was calculated by (V_{meas} – iR) – E (pH7.0) (where V_{meas} is the measured potential). To investigate the stability of all the samples, CV was repeated using a scan rate of 100 mV/s from 0.4 V to 1.5 V in 0.1 M phosphate buffer solution, after that LSV was recorded at a scan rate of 2 mV/s. Steady-state currents were collected at a variety of applied potentials starting at 1.2 V and proceeding in 10-20 mV steps to 0.98 V with rotating rate of 1600 rpm. The resistance collected was used to correct the Tafel plot for iR drop. The electrochemical measurements were also carried out in 0.04 M borate buffer solution (pH 9.0) according to the procedure above in phosphate buffer solution.

Single-Crystal Structure Determination

Single-crystal X-ray diffraction analyse was performed on a Rigaku Mercury CCD diffractometer (**1**). The diffractometer was equipped with graphite-monochromated Mo Kα radiation (λ = 0.7107 Å). Intensity data were collected by the narrow-frame method at 293 K. The data sets were corrected for Lorentz and polarization factors as well as for absorption by the multi-scan method.[S4] Structure was solved by direct methods and refined by full-matrix least-squares fitting on F^2 by SHELX-97.[S5] All non-hydrogen atoms were refined with anisotropic thermal parameters. All hydrogen atoms bonded to carbon and nitrogen atoms were located at geometrically calculated positions and refined with isotropic thermal parameters. The details of crystallographic data and selected bond lengths for the two compounds are summarized in Tables S1and S2.

Synthesis of Compound 1

Compound **1** was synthesized as follows: a mixture of $Co(NO_3)_2 \cdot 6H_2O$ (0.179 g, 0.6 mmol), S-H_3L (0.100 g, 0.48 mmol), and 2,2'-bipyridine (0.032 g, 0.20 mmol) in 5 mL of deionized water, added with five drops of $(CH_3)_4NOH$, was sealed in a 23-mL Teflon-lined stainless steel autoclave, followed by heating at 170 °C for 120 h. The autoclave was then slowly cooled to room temperature. Pink plate crystals of S-H_3L-Co suitable for single-crystal X-ray diffraction analysis were isolated from the final reaction mixture by filtration, washed several times with deionized water, and dried in air at ambient temperature. Yield: 11% based on S-H_3L. The purity of the sample was confirmed by powder XRD and elemental analyses. Anal.Calcd for$C_{12}H_{26}N_2O_{14}P_2Co_3$: C, 21.80; H, 3.96; N, 4.24. Found: C, 21.22; H, 4.12; N, 4.48.

Synthesis of Compound 2

Compound **2** was synthesized according to the modified literature method.[S6] Briefly, $Co(NO_3)_2 \cdot 6H_2O$ (0.179 g, 0.6 mmol) and S-H_3L (0.100 g, 0.48 mmol) were added in 10 mL of deionized water which was further added with 0.5 mL of $(C_4H_9)_4NOH$. The mixture was then transferred into a 23-mL Teflon-lined stainless steel autoclave which was heated at 170 °C for 120 h. After the autoclave was cooled to room temperature, pink plate crystals were isolated from the final reaction mixture by filtration, washed several times with deionized water and dried in air at ambient temperature. Yield: 13% based on S-H_3L. Anal.Calcd for$C_{12}H_{28}N_2O_{15}P_2Co_3$: C, 21.22; H, 4.16; N, 4.13. Found: C, 20.85; H, 4.23; N,4.27.

Synthesis of Compound 3

Compound **3** was synthesized according to the modified literature method.[S7] A mixture of $Co(CH_3COO)_2{\cdot}4H_2O$ (0.455 g, 1.83mmol) and $PPAH_3$ (0.289 g, 1.83 mmol) in 10 mL of deionized water was sealed in a 23-mL Teflon-lined stainless steel autoclave followed by heating at 120 °C for 72 h. The autoclave was then slowly cooled to room temperature. Pink spherical crystals of PPA-Co were isolated from the final reaction mixture by filtration, washed several times with deionized water, and dried in air at ambient temperature. Yield: 11% based on $Co(CH_3COO)_2{\cdot}4H_2O$. Anal. Calcd for $C_6H_{20}O_{16}P_2Co_3$: C, 12.28; H, 3.43. Found: C, 12.50; O, 2.81.

Synthesis of Compound 4

Compound **4** was synthesized according to the modified literature method.[S8] A mixture of $CoCl_2$ (0.0713 g, 0.5 mmol) and PPH_3 (0.047 g, 0.3 mmol) in 10 mL of water, with three drops of $(CH_3)_4NOH$ added, was sealed in a 23-mL Teflon-lined stainless steel autoclave at 140 °C for 72 h. The autoclave was then slowly cooled to room temperature. Pink plate crystals of PP-Co were isolated from the final reaction mixture by filtration, washed several times with distilled water, and dried in air at ambient temperature. Yield: 11% based on S-H_3L. Anal. Calcd for $C_6H_7O_4PCo$: C, 30.93; H, 3.03. Found: C, 31.02; O, 2.916. In addition, **4** can also be synthesized using a mixture of $Co(CH_3COO)_2{\cdot}4H_2O$ (0.455 g, 1.83 mmol) and PPH_3 (0.295 g, 1.83 mmol) dissolved in 10 mL of water. After stirring for 10 min and sealed in 23-mL Teflon-lined stainless steel autoclave at 140 °C for 48 h, polycrystalline pure phase was obtained after cooling to room temperature.

Table S1. Summary of crystal data and structural refinements for **1.**

Compound	**1**
Formula	$C_{12}H_{26}N_2O_{14}P_2$ Co_3
Fw	661.08
Crystal system	Monoclinic
Space group	$C2/c$
a (Å)	23.446(10)
b (Å)	9.956(4)
c (Å)	19.018(8)
β(°)	98.983(5)
V (Å^3)	4385(3)
Z	8
D_{calcd}(g·cm^{-3})	2.003
F(000)	2680
μ(mm^{-1})	2.463
R_1, wR_2 [I>2σ(I)]^a	0.0462, 0.0939
R_1, wR_2 (all data)^a	0.0647, 0.1047

$^aR_1 = \Sigma||F_o| - |F_c||/\Sigma|F_o|$, $wR_2 = \{\Sigma w[(F_o)^2 - (F_c)^2]^2/\Sigma w[(F_o)^2]^2\}^{1/2}$.

Table S2. Selected bond length (Å) for **1**.[a]

1			
Co(1)-O(8)#1	2.006(3)	Co(3)-O(6)#1	2.149(3)
Co(1)-O(2)#2	2.089(3)	Co(3)-O(4W)	2.191(3)
Co(1)-O(5)	2.108(3)	Co(3)-O(5)	2.199(3)
Co(1)-O(2W)	2.155(3)	O(4)-C(6)	1.250(4)
Co(1)-O(2)	2.165(3)	O(5)-C(6)	1.269(4)
Co(1)-N(1)	2.209(3)	O(9)-C(12)	1.257(6)
Co(2)-O(1)	2.034(3)	O(10)-C(12)	1.257(5)
Co(2)-O(10)	2.059(3)	P(1)-O(1)	1.511(3)
Co(2)-O(7)	2.090(3)	P(1)-O(3)	1.512(3)
Co(2)-O(7)#3	2.120(3)	P(1)-O(2)	1.543(3)
Co(2)-O(1W)	2.142(3)	P(1)-C(5)	1.813(3)
Co(2)-N(2)	2.256(4)	P(2)-O(8)	1.505(3)
Co(3)-O(3)#2	2.028(3)	P(2)-O(6)	1.527(3)
Co(3)-O(3W)	2.082(3)	P(2)-O(7)	1.531(3)
Co(3)-O(6)#4	2.119(3)	P(2)-C(11)	1.820(4)

[a] Symmetry code to generate equivalent atoms:#1 x,-y+1,z+1/2; #2 -x+1,y,-z+1/2; #3 -x+1,-y+1,-z; #4 -x+1,y-1,-z+1/2.

Table S3. Hydrogen bond distances (Å) and angles (°) for **1**.

D-H...A	d(D-H)	d(H...A)	d(D...A)	<(DHA)
O(1W)-(1WB)...O(4W)#5	0.85	1.87	2.715(4)	173.8
O(2W)-H(2WA)...O(9)#1	0.85	1.88	2.725(5)	178.8
O(4W)-H(4WB)...O(4)#2	0.85	2.01	2.844(5)	165.7

Symmetry transformations used to generate equivalent atoms:

#1 x,-y+1,z+1/2; #2 -x+1,y,-z-1/2; #5 -x+1,y+1,-z-1/2.

Table S4. Water oxidation activities of cobalt phosphonate catalysts.

Catalyst	**TOF × 10^3 (s^{-1})**[a]	**TOF (µmol s^{-1} m^{-2})**[b]	**TON**[c]	**Yield (%)**[d]	**BET (m^2 g^{-1})**	**Bond length standard deviation(δ)**[e]
1	5.16±0.02	0.30±0.02	10±2	78±2	23	0.0659
2	3.81±0.02	0.29±0.02	9±2	77±2	20	0.0573
3	3.21±0.03	0.19±0.03	6±1	57±2	26	0.0524
4	0.89±0.03	0.05±0.03	2±1	40±1	81	0.0778
Co_3O_4	0.51±0.03	0.03±2	1	21±1	74	
Co_3O_4[e]	1.14[f]	0.14[f]		64[f]	34[f]	

[a] Turnover frequency defined as O_2 evolution rates after 10 min of photo-irradiation/catalyst amount.

[b] Apparent turnover frequency defined as O_2 evolution rates after 10 min of photoirradiation/catalyst weight/specific surface area.

[c] TON defined as the amount of oxygen evolved/the amount of catalyst.

[d] Yield = (mole of O_2)/(1/2×mol of $Na_2S_2O_8$).

[e] $\delta = \sqrt{\frac{\sum (l_i - l_0)^2}{i}}$, l_i, referred to as Co-X(X = O, or/and N) distances; l_0, averaged Co-X(X = O,N)bond distance. i, the total amount of Co-X(X = O,N)bond.

[f] Data from Ref S9.

Table S5. The pH values of the photocatalytic system after photocatalysis.[a]

Catalyst	pH value of borate buffer	Reaction time (min)	pH value after photocatalysis
1	9.0	80	8.63
2	9.0	80	8.65
3	9.0	80	8.64
4	9.0	80	8.57

[a] Reaction condition: 0.14 g L^{-1} catalyst, 1.0 mM $[Ru(bpy)_3]^{2+}$, 5.0 mM $Na_2S_2O_8$, 40 mM borate buffer, total volume of the reaction solution 10 mL, light source: 300 W Xe lamp with 420 nm cut-off filter.

Table S6. Water oxidation activities of as-synthesized crystal cobalt phosphonate catalysts.

Catalyst	R_{O2} (μmol s^{-1} g^{-1})[a]	TOF × 10^3 (s^{-1})[b]	TOF (μmol s^{-1} m^{-2})[c]	Yield (%)[d]	BET (m^2 g^{-1})
1	5.1±0.4	3.41±0.04	1.13±0.03	57±2	4.6
2	4.8±0.3	3.27±0.03	0.89±0.03	50±1	5.4
3	3.7±0.2	2.15±0.02	0.57±0.03	41±2	6.4
4	2.3±0.4	0.52±0.04	0.15±0.03	23±3	14.9

[a] O_2 evolution rate (normalized by the catalyst mass) after irradiation for 10 min.

[b] Turnover frequency defined as O_2 evolution rate after 10 min of photo-irradiation/catalyst amount.

[c] Apparent turnover frequency defined as O_2 evolution rates after 10 min of photoirradiation/catalyst weight/specific surface area.

[d] Yield = (mole of O_2)/(1/2×mol of $Na_2S_2O_8$).

Reaction condition: as-synthesized crystal sample (0.14 g L^{-1}), 1.0 mM $[Ru(bpy)_3]^{2+}$, 5.0 mM $Na_2S_2O_8$, 40 mM borate buffer (initial pH 9.0), total volume of the reaction solution 10 mL, light source: 300 W Xe lamp with 420 nm cut-off filter.

Table S7. ICP-MS data for solution after photocatalytic reaction.[a]

Catalyst	Cobalt phosphonates (μM)	Reaction time (min)	Cobalt in reaction solution after centrifugation (μM)	Cobalt species dissolved in reaction solution (%)
1	535	80	31	1.9
2	552	80	38	2.3
3	537	80	25	1.5
4	515	80	12	2.3

[a] Reaction condition: 0.14 g L^{-1}catalyst, 1.0 mM $[Ru(bpy)_3]^{2+}$, 5.0 mM $Na_2S_2O_8$, 40 mM borate buffer (initial pH 9.0), total volume of the reaction solution 10 mL, light source: 300 W Xe lamp with 420 nm cut-off filter.

Table S8. Electrochemical properties of cobalt phosphonate catalysts.[a]

	100 mM phosphate buffer (pH 7)			40 mM Borate buffer (pH 9)	
Catalyst	Over-potential (η, mV)	Tafel slope (mV/decade)[a]	Tafel slope (mV/decade)[b]	Over-potential (η, mV)	Tafel slope (mV/decade)[b]
1	484	83±1	92±2	468	68
2	493	83±1	94±2	474	69
3	503	85±2	94±1	494	74
4	508	90±3	96±1	497	74
Co_3O_4	481	82±5	82±2	454	66
Co_3O_4[c]	480	88			

[a] Data were calculated from LSV.

[b] Data were calculated based on steady state data.

[c] Data from Ref. S10.

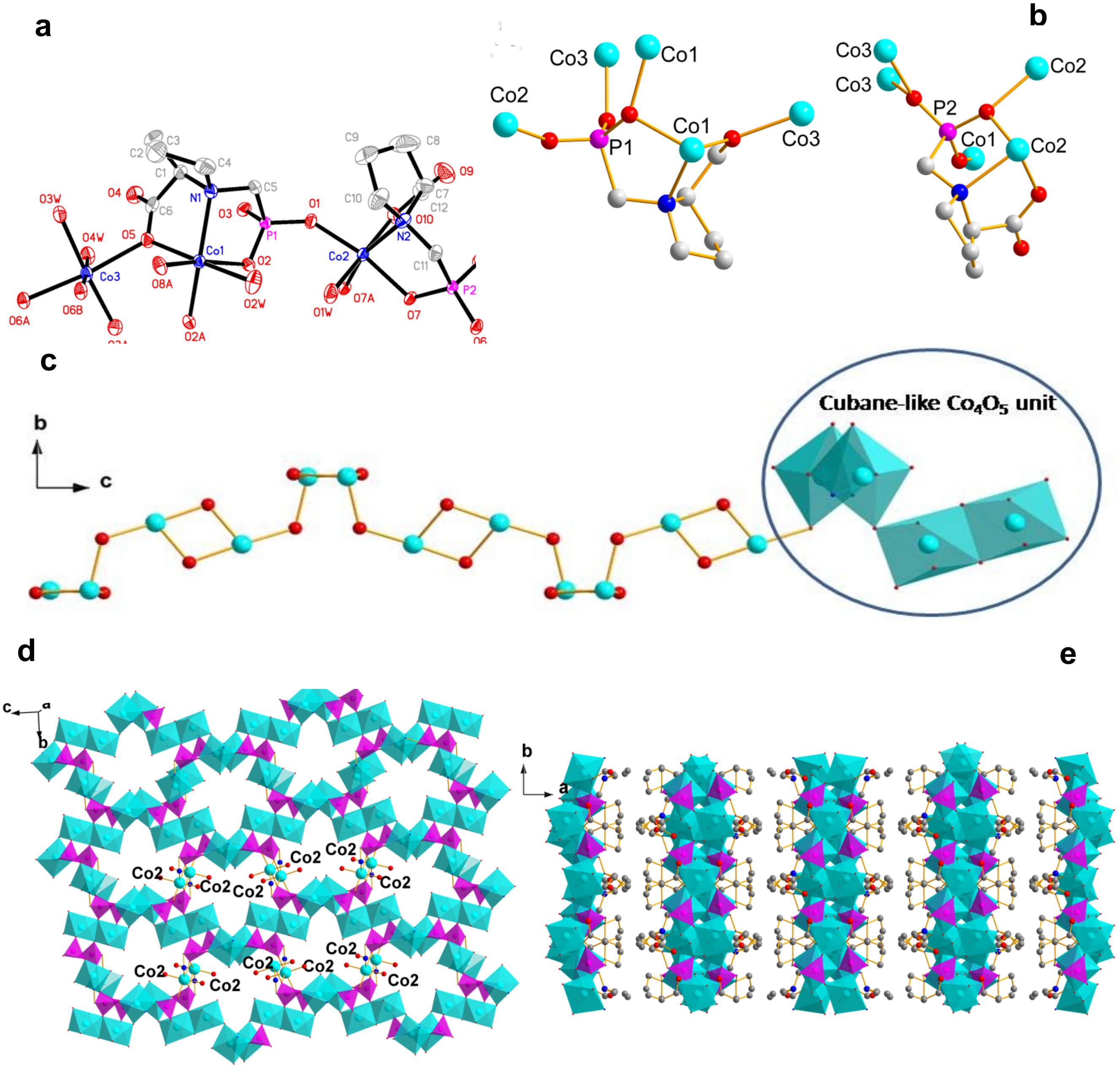

Fig. S1 (a) ORTEP drawing of the asymmetric unit in **1** with atomic labeling scheme. Thermal ellipsoids are at the 30% probability level. H atoms and lattice water molecules were omitted for clarity. (b) The coordination models of S-H_3L ligand in **1**. (c) Co-O chain consisting of cubane-like Co_4O_5 unit along the *c*-axis. (d) Inorganic layer of **1** in the *bc* plane. (e) Layered architecture of **1** along *c*-axis. Co, O, P, and N are shown as cyan, red, magenta, and blue circles, respectively. CoO_6, CoO_5N polydedra and CPO_3 tetrahedra are shaded in cyan and magenta, respectively.

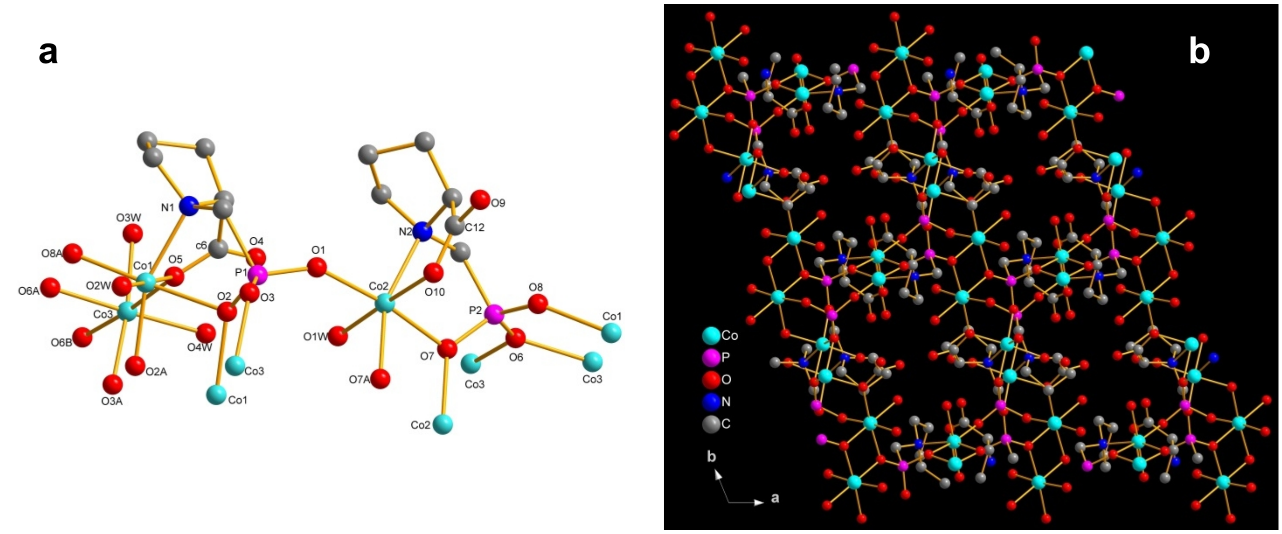

Fig. S2 (a) The coordination environment around cobalt(II) ion in **2**, and (b) crystal structural packing of **2** in the *ab* plane. CIF file was obtained from Cambridge Crystallographic *Data* Centre (*CCDC*199770).

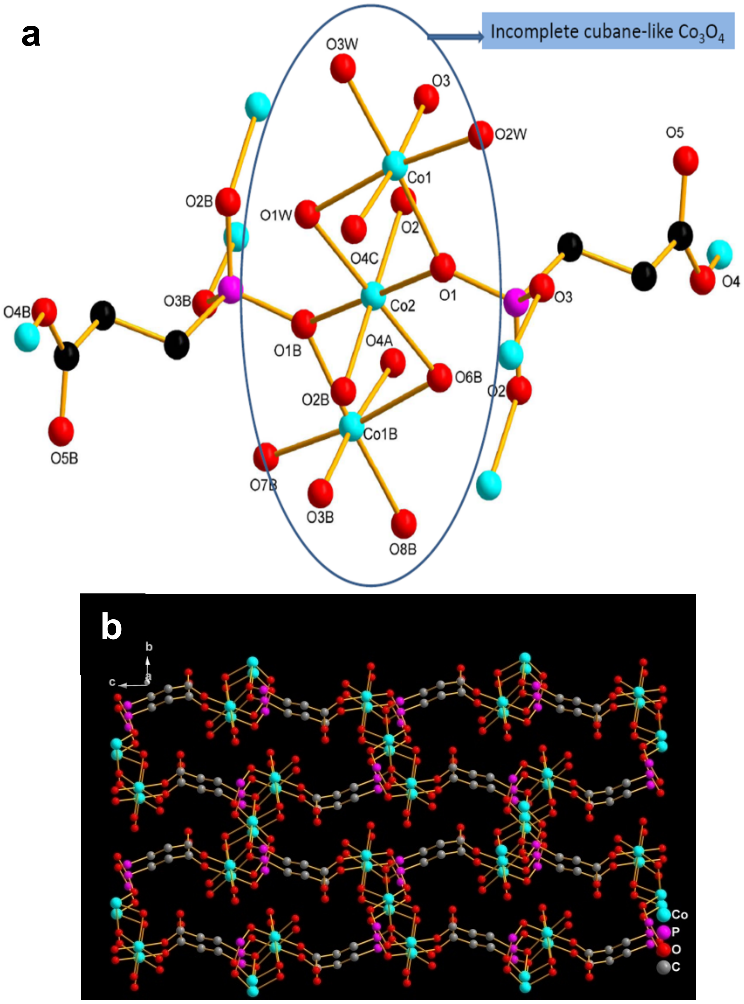

Fig. S3 (a) The coordination environment around cobalt(II) ion in **3**, and (b) crystal structural packing of **3** in the *bc* plane. CIF file was obtained from Cambridge Crystallographic *Data* Centre (WebCSD:SOMQUG).

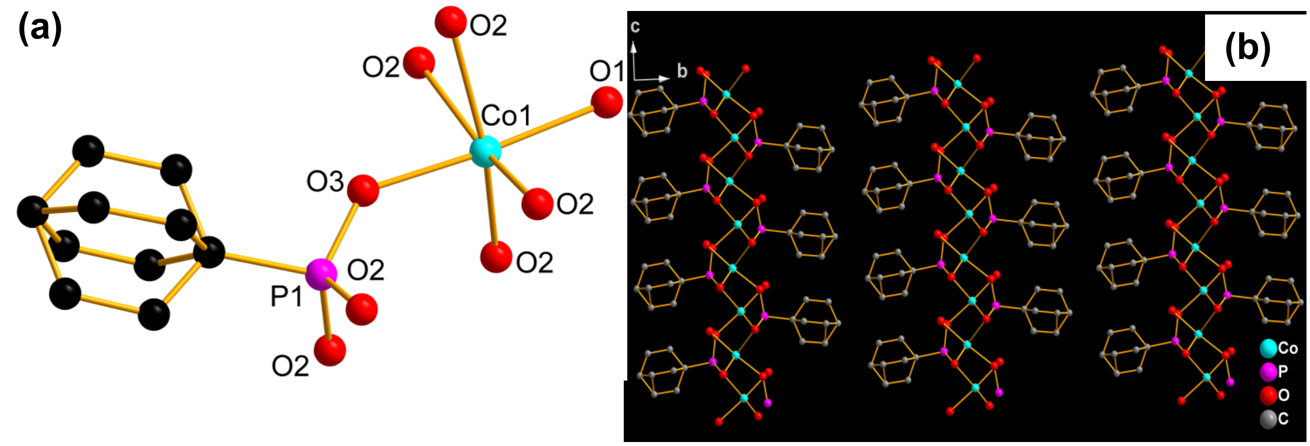

Fig. S4 (a) The coordination environment around cobalt(II) ion in **4**, and (b) Crystal structural packing of Compound **4** in the *ab* plane. CIF file was obtained from Cambridge Crystallographic Data Centre (CCDC 279873).

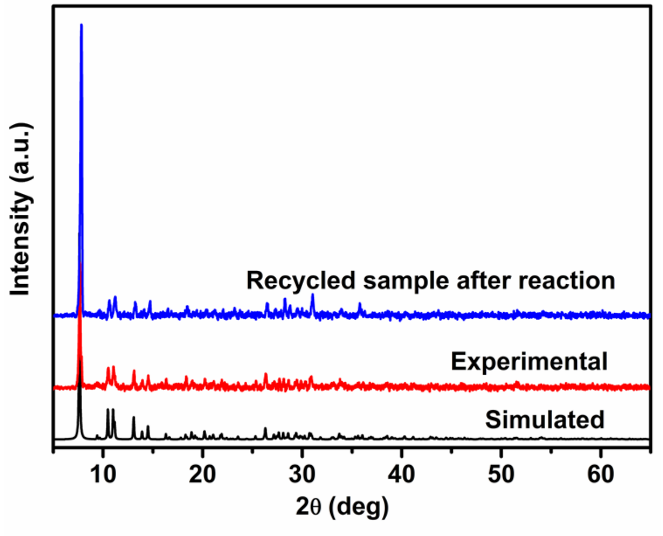

Fig. S5 Simulated and experimental XRD powder patterns for **1**.

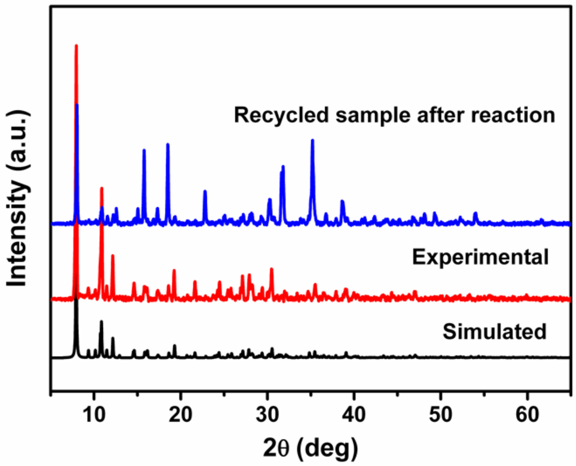

Fig. S6 Simulated and experimental XRD powder patterns for **2**.

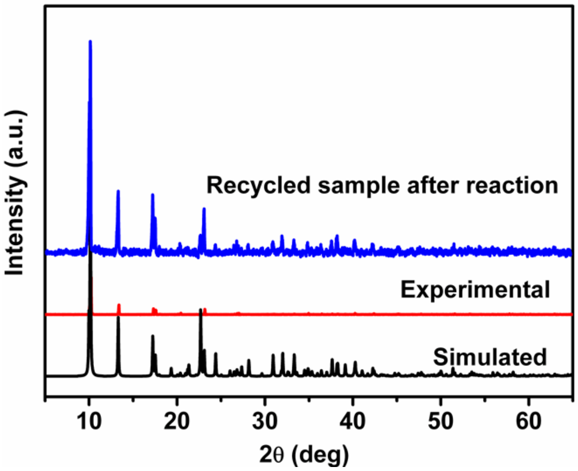

Fig. S7 Simulated and experimental XRD powder patterns for **3**.

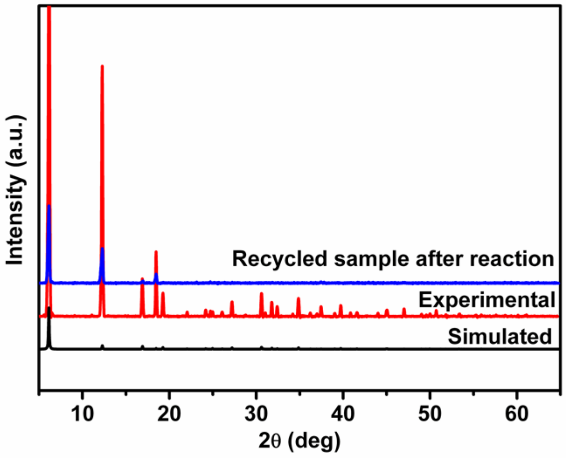

Fig. S8 Simulated and experimental XRD powder patterns for **4**.

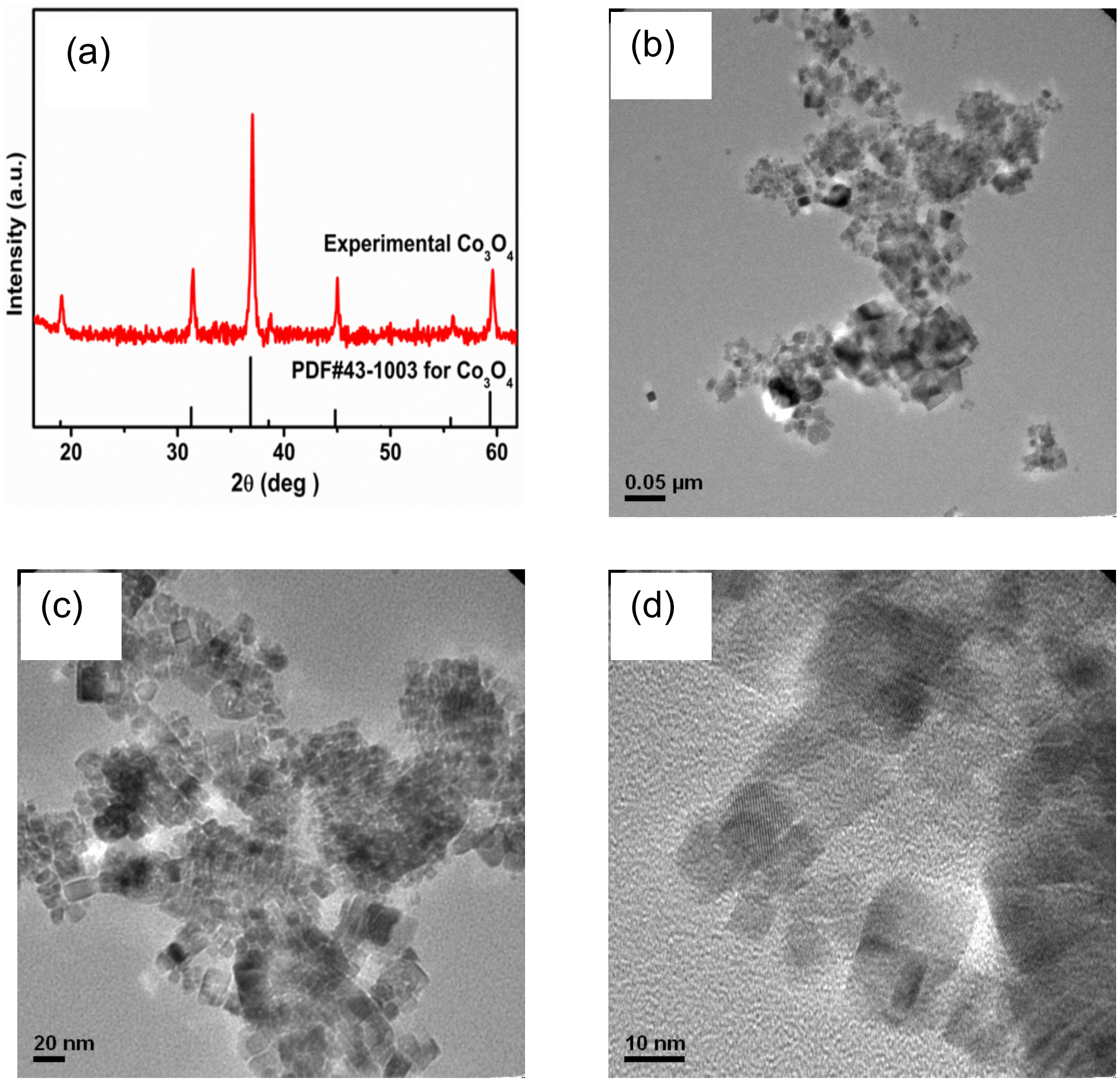

Fig. S9 Standard line pattern (PDF#43-1003) and experimental XRD powder pattern (a), and TEM images (b, c, d) of Co_3O_4.

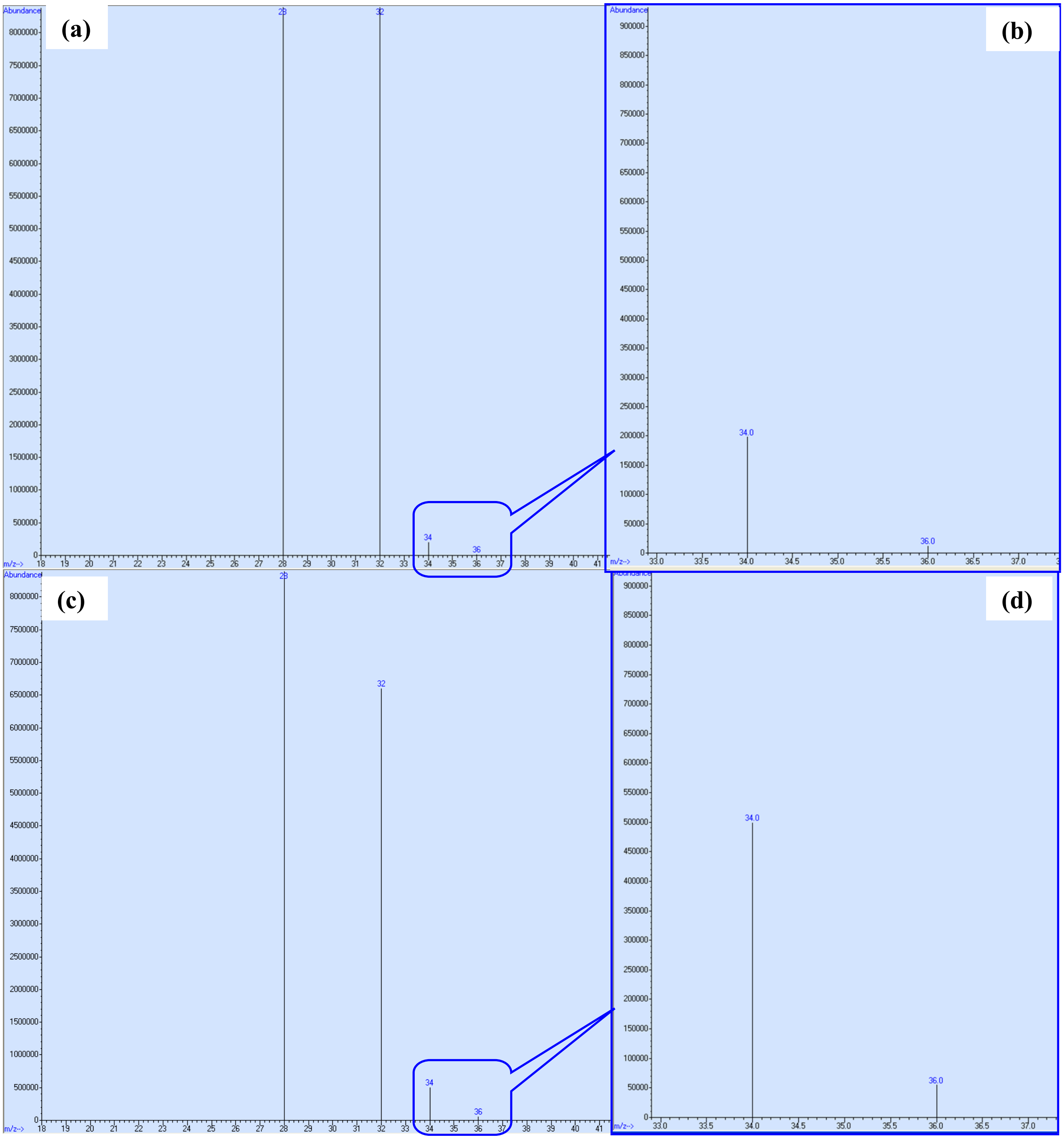

Fig. S10 EI mass spectrum of air (100 μL) (*a*, *b*) and the gas sample evolved (100μL) (*c*, *d*) during photocatalysis using sample **1** in$^{18}OH_2$-enriched borate buffer solution (16.8%,$^{18}OH_2$).

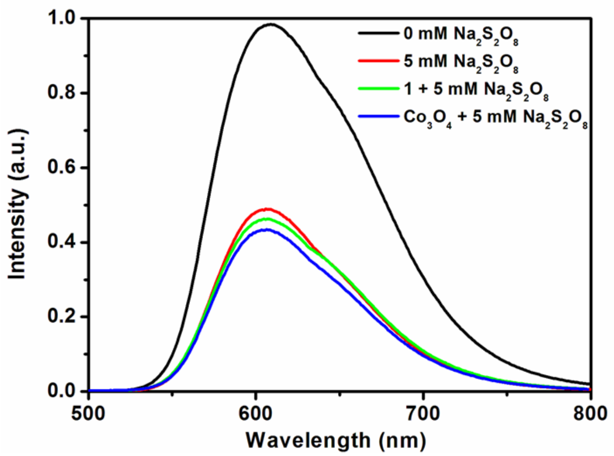

Fig. S11 Steady-state luminescence spectra of $[Ru(bpy)_3]^{2+}$ in the presence and absence of 5.0 mM persulfate; and in the presence of 5.0 mM persulfate and the catalyst (**1** and Co_3O_4) (λ_{ex} = 450 nm). Conditions: 1.0 mM $[Ru(bpy)_3]^{2+}$, 40 mM borate buffer (initial pH 9.0), 0.14 g L^{-1} catalyst.

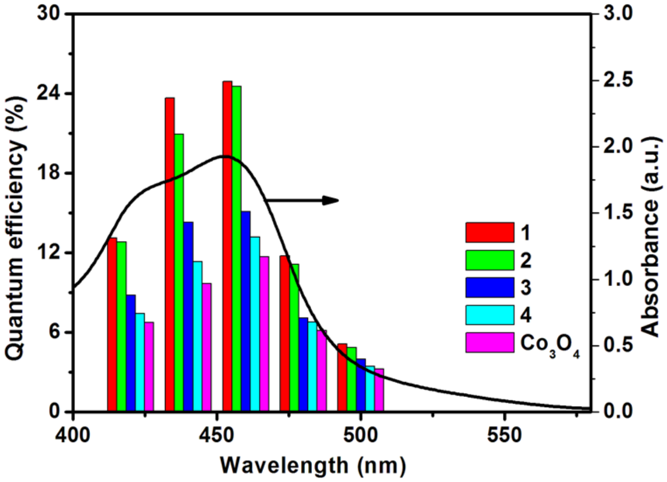

Fig. S12 The quantum efficiencies of O_2 evolved under light-irradiation at different wavelength of 420, 440, 460, 480, and 500 nm over different cobalt phosphonates (**1-4)** and Co_3O_4 control (0.14 g L^{-1}) and UV-vis absorption spectrum of $Ru(bpy)_3Cl_2$. Conditions: 1.0 mM $[Ru(bpy)_3]^{2+}$, 5.0 mM $Na_2S_2O_8$, 40 mM borate buffer (initial pH 9.0), total volume of the reaction solution 100 mL, light source: 300 W Xe lamp with different wavelength cut-off filter. It is to note that only a small amount of oxygen was generated with the band-pass filter. To obtain more accurately data, the total reaction solution volume was increase to 100 mL with other conditions kept the same.

Comments:

In the water oxidation system using $[Ru(bpy)_3]^{2+}$ as a photosensitizer and $Na_2S_2O_8$ as a two-electron acceptor, the overall reaction can be expressed as:

$$2H_2O + 2Na_2S_2O_8 \rightarrow O_2 + 4H^+ + 4Na^+ + 4SO_4^{2-} \qquad (1)$$

This suggests that in any condition, the theoretical maximum amount of O_2 produced should correspond to half of the amount of persulfate added.

During photocatalytic water oxidation, the photoexcitation of $[Ru(bpy)_3]^{2+}$ generates $[Ru(bpy)_3]^{3+}$ by the oxidative quenching of the metal-ligand charge-transfer (MLCT) excited state $[Ru(bpy)_3]^{2+*}$ with $Na_2S_2O_8$. The absorption of two photons and the consumption of 2 equiv. of $Na_2S_2O_8$ results in the formation of 4 equiv. of $Ru(bpy)_3]^{3+}$ as shown in equation (2). Hence, the quantum efficiency of O_2 formation is defined as the number of O_2 molecules formed per two absorbed photons.

$$4[Ru(bpy)_3]^{2+} + 2Na_2S_2O_8 + 2h\nu \rightarrow 4Ru(bpy)_3]^{3+} + 4Na^+ + 4SO_4^{2-} \qquad (2)$$

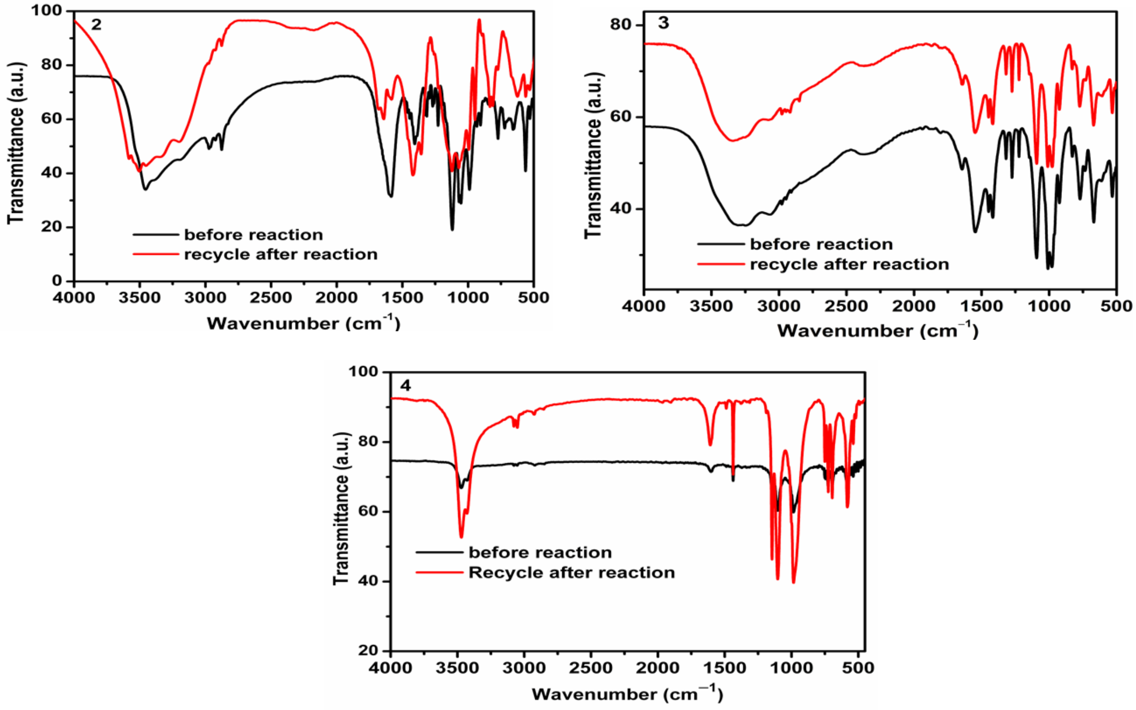

Fig. S13 FTIR spectra of cobalt phosphonates before and after photoreaction.

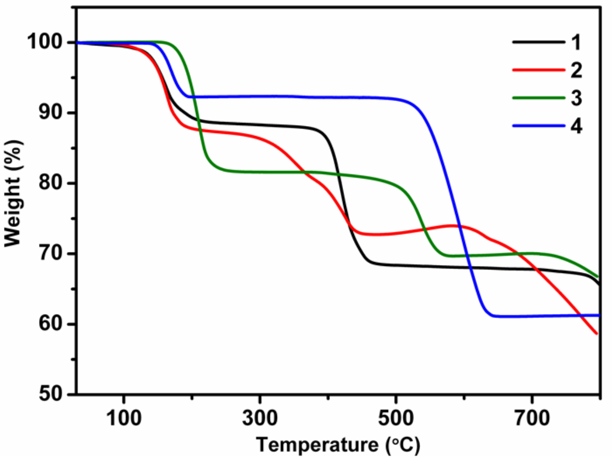

Fig. S14 TGA results of cobalt phosphonates.

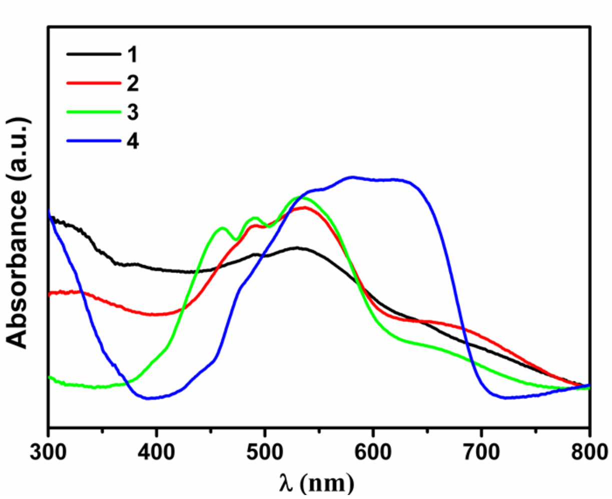

Fig. S15 UV-Vis diffuse reflectance spectra (DRS).

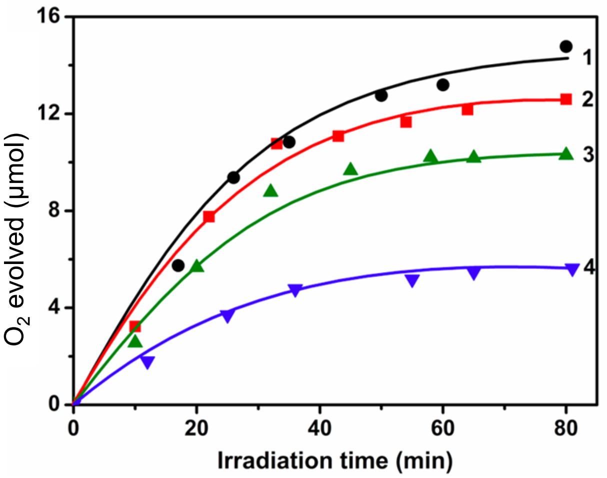

Fig. S16 O_2 production over the as-synthesized crystal samples **1-4** without grinding (0.14 g L^{-1}). Conditions: 1.0 mM $[Ru(bpy)_3]^{2+}$, 5.0 mM $Na_2S_2O_8$, 40 mM borate buffer (initial pH 9.0), total volume of the reaction solution 10 mL, light source: 300 W Xe lamp with 420 nm cut-off filter.

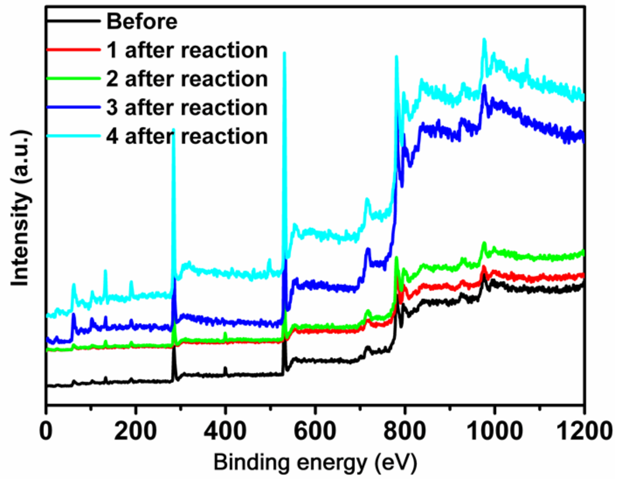

Fig. S17 XPS survey scans of **1-4** after photocatalytic reaction and **1** before reaction.

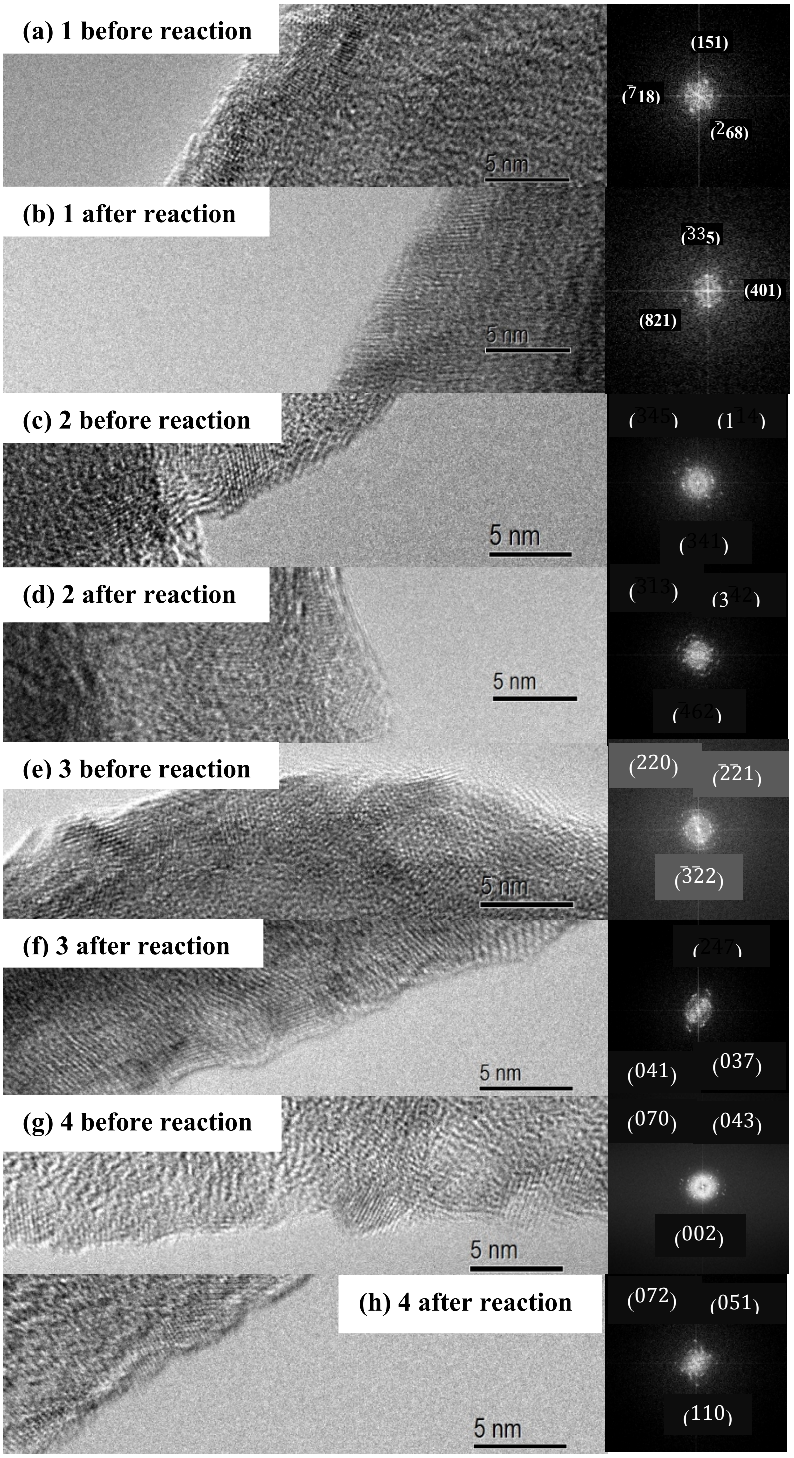

Fig. S18 HRTEM images (left) and FFTs (right) of surface regions of **1-4** before and after photocatalysis. Photocatalytic reaction conditions: cobalt phosphonates **1-4** (0.14 g L^{-1}), 1.0 mM $[Ru(bpy)_3]^{2+}$, 5.0 mM $Na_2S_2O_8$, 40 mM borate buffer (initial pH 9.0), total volume of the reaction solution 10 mL, light source: 300 W Xe lamp with 420 nm cut-off filter.

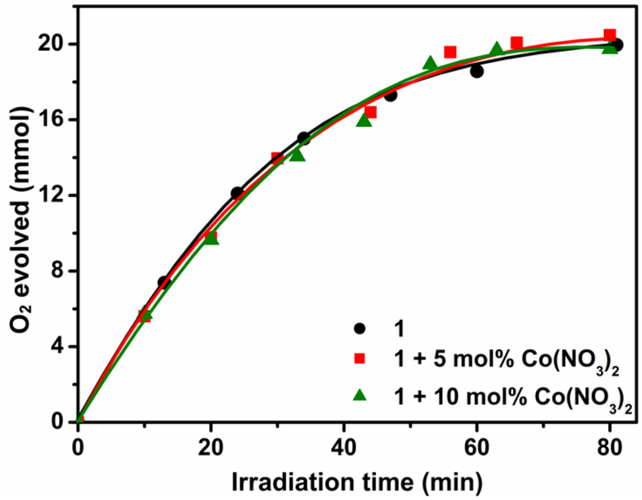

Fig. S19 O_2 evolution over **1** (0.14 g L^{-1}), and the mixture of **1** and $Co(NO_3)_2$. Conditions: 1.0 mM $[Ru(bpy)_3]^{2+}$, 5.0 mM $Na_2S_2O_8$, 40 m Mborate buffer (initial pH 9.0), total volume of the reaction solution 10 mL, light source: 300 W Xe lamp with 420 nm cut-off filter.

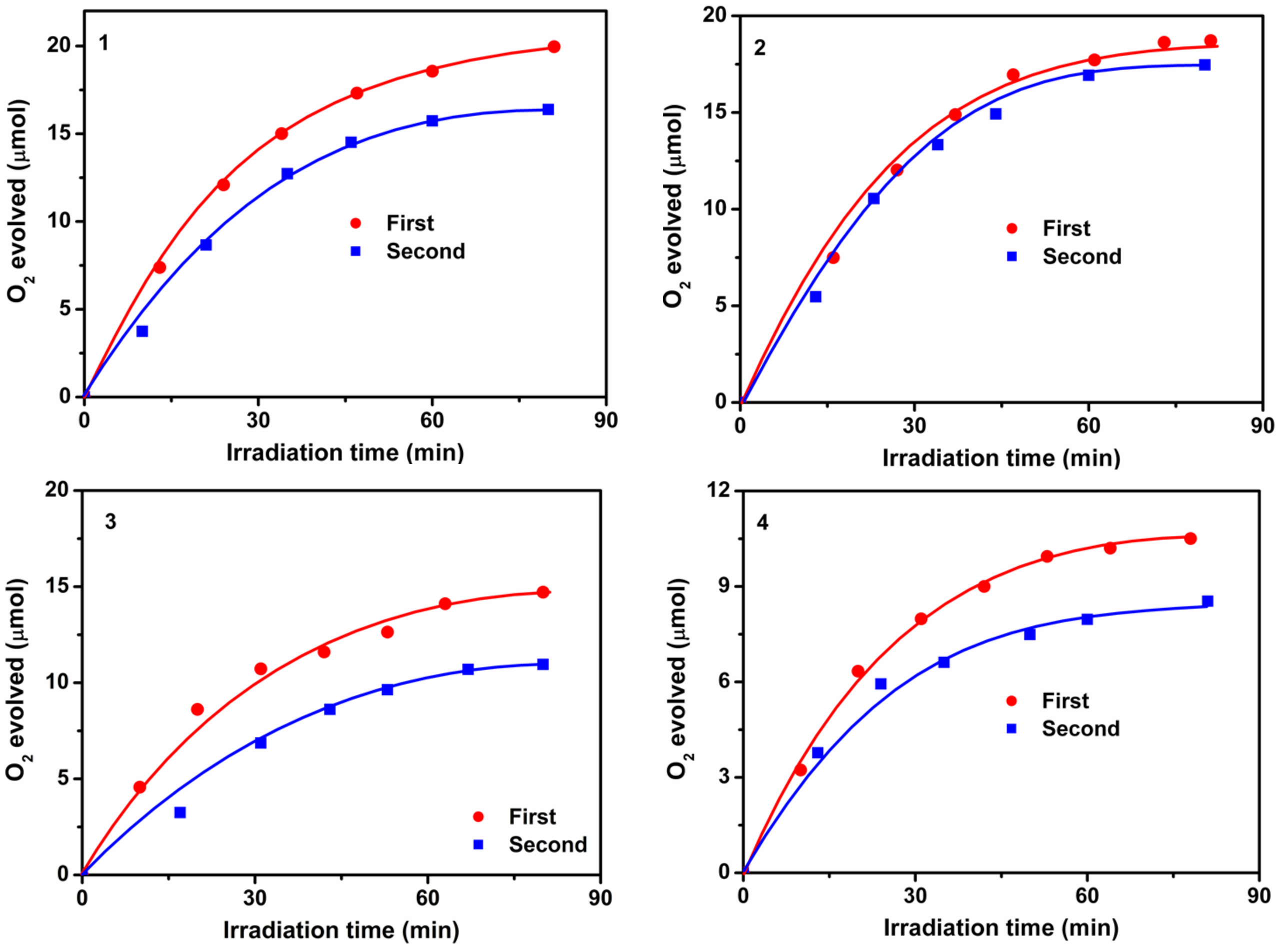

Fig. S20 O_2 production over the fresh sample and recycled sample of **1-4** (0.14 g L^{-1}). Conditions: 1.0 mM $[Ru(bpy)_3]^{2+}$, 5.0 mM $Na_2S_2O_8$, 40 mM borate buffer (initial pH 9.0), total volume of the reaction solution 10 mL, light source: 300 W Xe lamp with 420 nm cut-off filter.

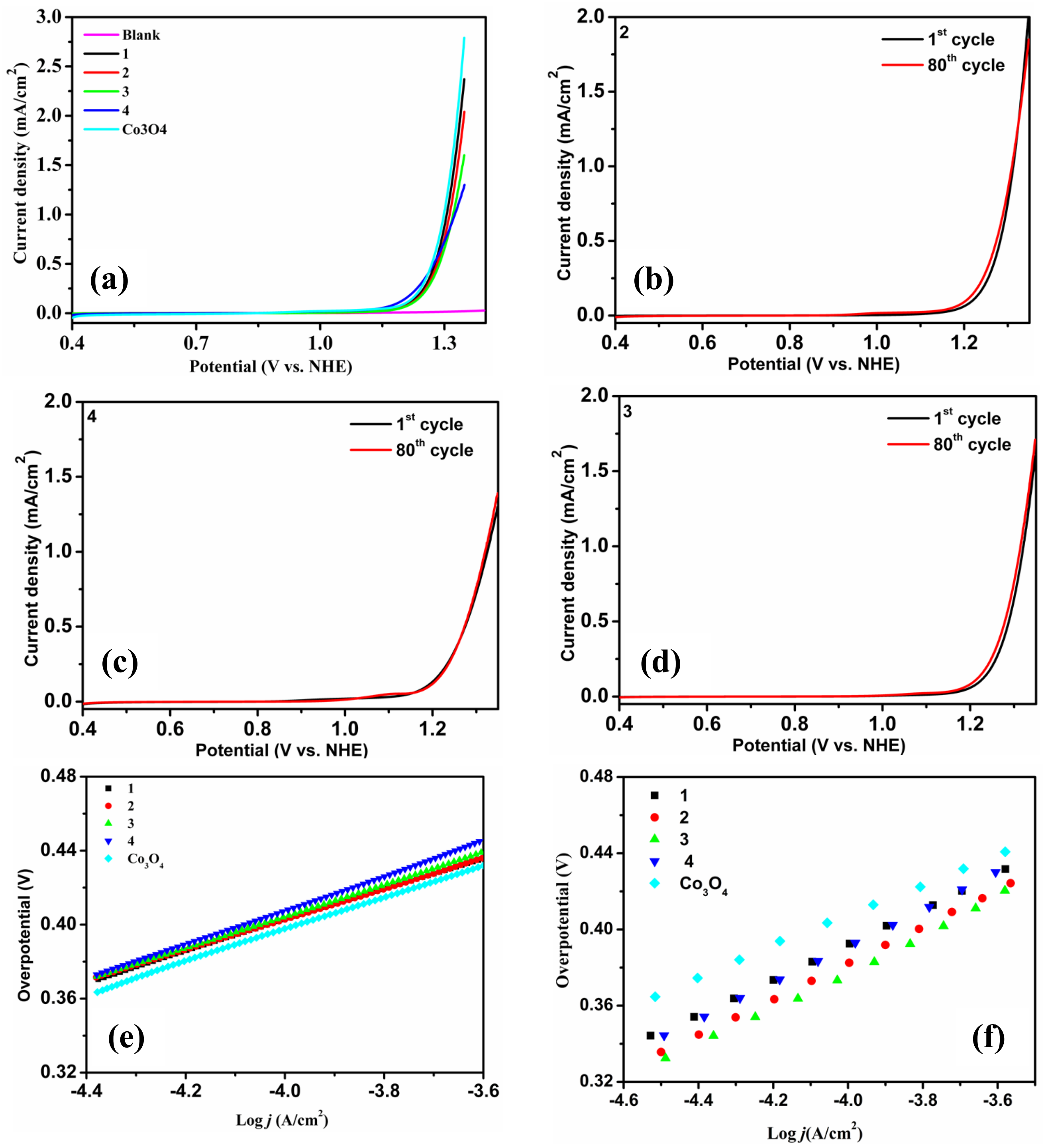

Fig. S21 (a) LSV curves of layered cobalt phosphonates and control Co_3O_4, LSV curves of 2 (b), 3 (c), and 4 (d) showing the first and 80th cycles, and Tafel plots obtained by LSV (e) and steady state data (f). All results were obtained in 0.1 M phosphate buffer solution (pH 7.0).

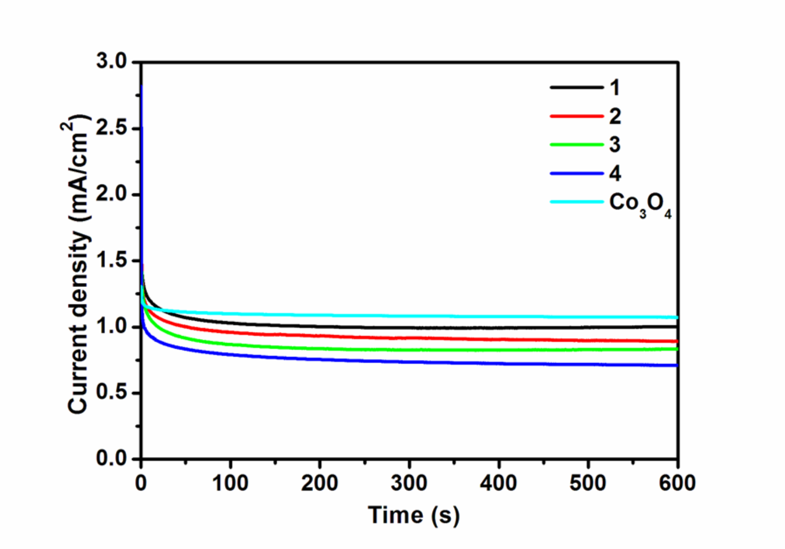

Fig. S22 Chronoamperometric *i*-t curves obtained with cobalt phosphonates modified glass carbon electrodes. Electrolysis experiments were carried out in 0.1 M phosphate buffer solution (pH 7.0) at a constant applied potential of +1.3 V versus NHE. During the measurement, the electrode was rotated at a rate of 1600 rpm to remove O_2 bubbles formed from the electrode surface and the pH was remained unchanged in the longer timescale experiments.

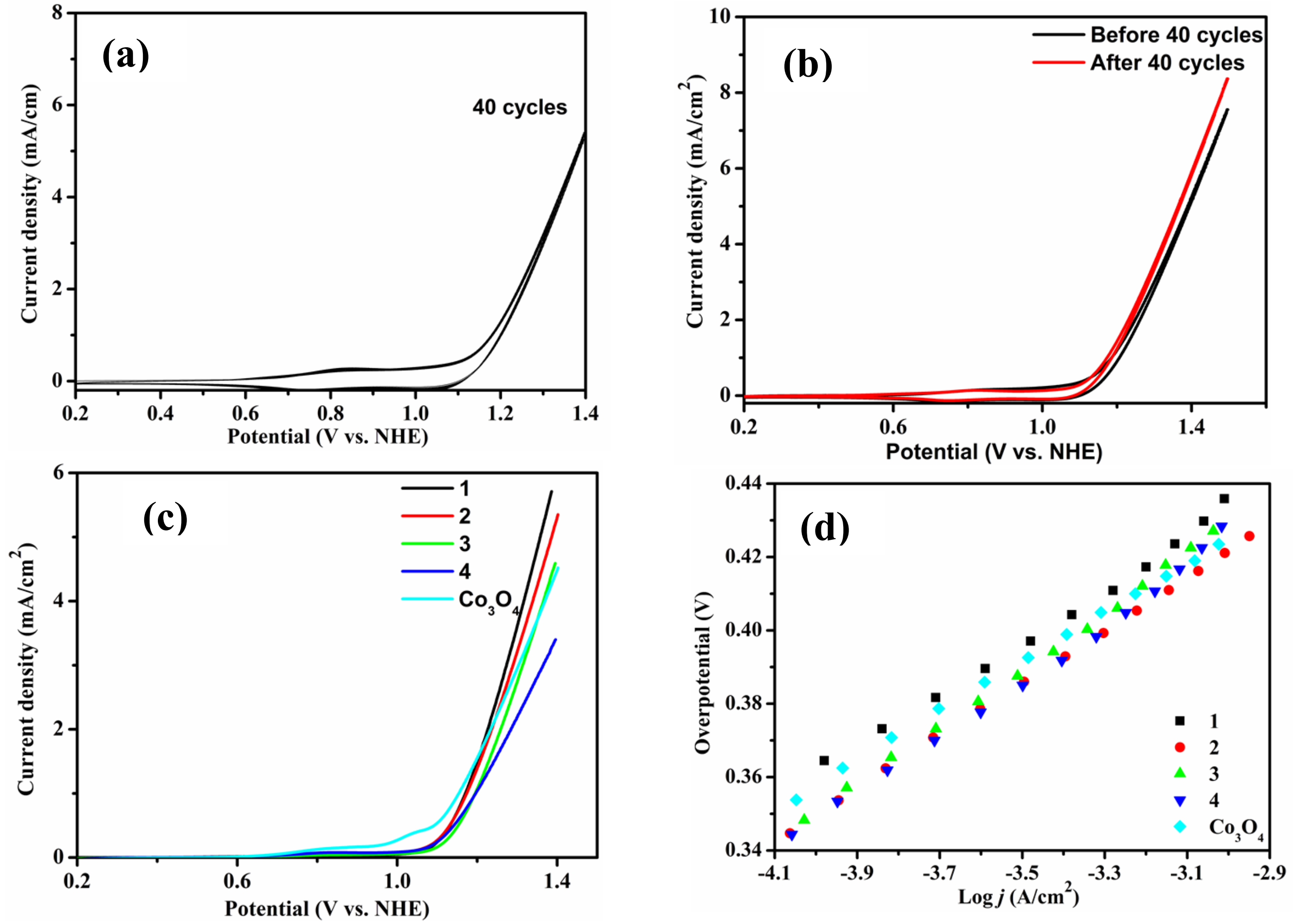

Fig. S23 (a) CV scans of **1** from 0.2 to 1.4 V at a scan rate of 100 mV/s for continuous cycles, (b) CVs of **1** at a scan rate of 20 mV/s from 0.2 to 1.5 V before and after 40 continuous cycles, (c) LSV curves of **1**-**4** and Co_3O_4, and (d) Tafel plots obtained from steady state data. All results were obtained at 1600 rpm in 40m Mborate (pH 9.0).

References

S1. B. P. Yang, J. G.Mao, Y. Q. Sun, H. H. Zhao, Clearfield, A. *Eur. J. Inorg. Chem.*2003, 4211-4217.

S2. Y. Liang, Y. Li, H. Wang, J. Zhou, J. Wang. T. Regier, H. Dai, *Nat. Mater.*2011,**10**, 780-786.

S3. S. Yusuf, F. Jiao, *ACS Catal.*2012,**2**, 2753-2760.

S4. CrystalClear v. version 1.3.5 (Rigaku Corp, Woodlands, TX, 1999).

S5. SHELXTL, Crystallographic Software Package version 5. 1 (Bruker-AXS, Madison, WI, 1998).

S6. A. Turner, P.-A. Jaffres, E. J. MacLean, D. Villemin, V. McKee, G. B. Hix, *Dalton Trans.* 2003, 1314-1319.

S7. A. Distler, S.C. Sevov,*Chem. Commun.*1998,959-960.

S8. T.Q. Salami, X. Fan, P.Y.Zavalij, S. R. J. Oliver, *Dalton Trans*, 2006,1574-1578.

S9. D. Hong, Y. Yamada, T. Nagatomi, Y.Takai, S.Fukuzumi, *J. Am. Chem. Soc.*2012, **134**, 19572.

S10. T. W. Kim, M. A. Woo, M. Regis and K.-S. Choi, *J. Phys. Chem. Lett.*, 2014, 13, 2370-2374.